Advanced Composite Materials
Publication details, including instructions for authors and subscription information:
http://www.tandfonline.com/loi/tacm20

Inter-fiber sliding in fabric shaping process

Yutaka Arimitsu , Shichiro Takahashi & Tsu-Wei Chou

Version of record first published: 02 Apr 2012.

To cite this article: Yutaka Arimitsu , Shichiro Takahashi & Tsu-Wei Chou (2003): Inter-fiber sliding in fabric shaping process , Advanced Composite Materials, 12:1, 23-34

To link to this article: http://dx.doi.org/10.1163/156855103322320356

Adv. Composite Mater., Vol. 12, No. 1, pp. 23–34 (2003)

Inter-fiber sliding in fabric shaping process

YUTAKA ARIMITSU [1,*], SHICHIRO TAKAHASHI [1] and TSU-WEI CHOU [2]

[1] *Department of Mechanical Engineering, Ehime University, 3 Bunkyo-cho, Matsuyama 790-8577, Japan*

[2] *Department of Mechanical Engineering, University of Delaware, Newark, Delaware 19716-3140, USA*

Received 31 May 2002; accepted 22 January 2003

Abstract—In the fabric shaping process during resin transfer molding, fabrics are deformed due to inter-fiber sliding and buckling of yarns. We have observed inter-fiber sliding and yarn buckling in the deep drawing of fabrics by a cylindrical punch. The amount of punch traveling and the molding die radius affect the occurrence of inter-fiber sliding and yarn buckling. Comparing simulation results and actual deformation of fabrics, we should take account of inter-fiber-sliding and buckling of yarns.

Keywords: Resin transfer molding; textile composite; fabric shaping; inter-fiber sliding.

1. INTRODUCTION

Resin transfer molding is widely employed to produce thin-walled composite structures. An important topic in this field is formability of fabrics. Fabric deformation is sensitive to fabric types, initial orientation of yarns and the shape of the tools. Orientation of yarns after shaping and type of stitches of the fabrics affect the fluidity of injected resin and the resulting mechanical properties of the composite. Buckling of yarns and inter-fiber sliding also affect the strength of the composite shell and the deformation of fabrics, respectively. To predict these properties, simulation of the fabric shaping process is required in order to better understand the material performance.

The approaches to analyzing fabric draping and shaping can be classified into two categories. One is the geometrical approach through meshing of the curved surface; for example, the fishnet algorithm [1, 2], and meshing with a Computer Aided Design (CAD) system [3, 4]. The other is the mechanical approach through minimizing elastic energy of fabrics; for example, the Finite Element Method (FEM) using two-dimensional elements [5, 6], and modeling of fabrics using truss

*To whom correspondence should be addressed. E-mail: arimitsu@eng.ehime-u.ac.jp

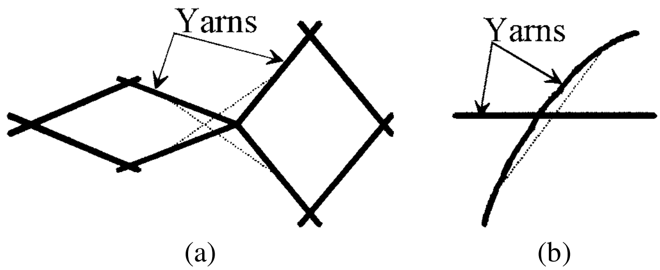

Figure 1. Patterns of inter-fiber sliding. (a) Large shear angle variation; (b) Single yarn bending.

(one-dimensional) elements [7]. In most studies of fabric draping/shaping, the pin-jointed network model (geometrical approach and modeling with one-dimensional elements) has been widely used. Also, no inter-fiber sliding was assumed in the FEM analysis with two-dimensional elements. Since inter-fiber sliding and yarn buckling are generally ignored in these simulation schemes, we need to investigate the assumptions made in neglecting these effects.

Recently, Lai and Young [8] proposed the modeling of fiber slippage using FEM. In their model, the amount of fiber slippage is geometrically estimated from the yarn curvature. They examined the effects of inter-fiber sliding experimentally, and reported that slippage became large near sharp corners.

Overall, yarn sliding has been observed in regions where the rate of shear angle variation is higher (see Fig. 1a), and where single yarn bending occurs (see Fig. 1b) [4]. In this paper, we determine experimentally the inter-fiber sliding and buckling of yarns, and measure the amount of inter-fiber sliding. The data obtained will be utilized to improve the simulation scheme of FEM with the pin-jointed network model [7].

2. DEEP DRAWING OF FABRICS

2.1. Test apparatus

We studied the effects of inter-fiber sliding by deep drawing with the cylindrical punch shown schematically in Fig. 2. We also employed semi-spherical punches (diameter: 30, 34 mm) to evaluate the effect of shapes of punches. A distributed load of 50 N is applied to the fabric by the blank-holder, and petroleum jelly is applied on contact surfaces with fabrics.

In the present research, the depth h and the radius r_2 of the molding die are important. The area of side surface is proportional to the punch traveling distance; but the region entering from the fringe on blank-holder to the side surface of a punch, increases rapidly with the punch traveling distance. Consequently, fabric area reduction occurs in the deep drawing process. The radius of the molding die determines the transition area of fabrics from the fringe to the side surface. It is expected that a large radius, r_2, of the molding die effects smooth deformation of fabrics from the fringe to the side surface of the cylinder.

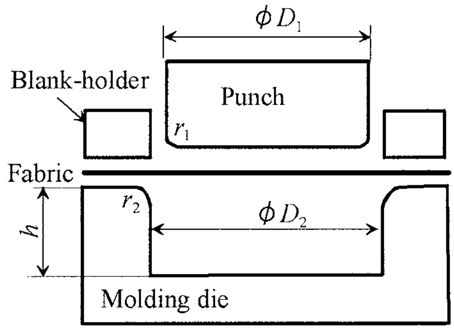

$D_1 = 30, 34$ mm, $D_2 = 32, 36$ mm,

$h = 10, 20, 26$ mm, $r_1 = 0.5$ mm, $r_2 = 2, 10$ mm

Figure 2. Deep drawing with cylindrical punch.

Table 1.
Characteristics of fabrics

Material	Thickness (mm)	Spacing of warp (mm)	Spacing of weft (mm)
Rayon	0.25	1.6	1.9

2.2. Test fabrics

Plain-weave rayon fabric of 100×100 mm^2 was used in this test. Their microstructural parameters are listed in Table 1. We employed fibers of 0.15 mm in diameter, to minimize the effect of waviness of woven fabrics.

Before fabric shaping, the intersections of yarns were marked by oil-based ink. Then, the inter-fiber sliding as indicated by the distance between the mark and the intersection of yarns after the fabric shaping process was measured.

3. DEFORMATION OF FABRICS

The deformation of plain-woven fabrics due to a cylindrical punch is shown in Figs 3–6. In deep drawing by a cylindrical punch, stitches of fabrics maintain their initial orientation and spacing on the basal surface of the punch. Large shear deformation is observed on the side surface of the cylindrical punch and the blank-holder surface (see Fig. 3). Inter-fiber sliding is negligibly small when the punch traveling distance h is small (see Fig. 4). Buckling of yarn by compression is observed on the side surface when the punch traveling h is large and the radius r_2 of a molding die is small (see Fig. 5). Inter-fiber sliding is also observed on the side surface when h is large and r_2 is small (see Fig. 6). On the other hand, inter-fiber sliding in deep drawing with a semi-spherical punch is negligibly small.

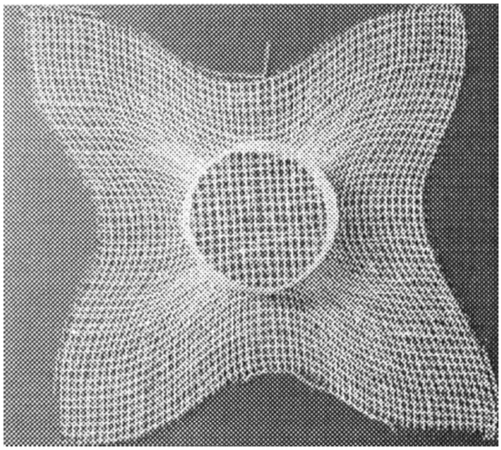

Figure 3. Fabric deformation of deep drawing, $D_1 = 30$ mm, $D_2 = 32$ mm, $h = 20$ mm, $r_2 = 2$ mm.

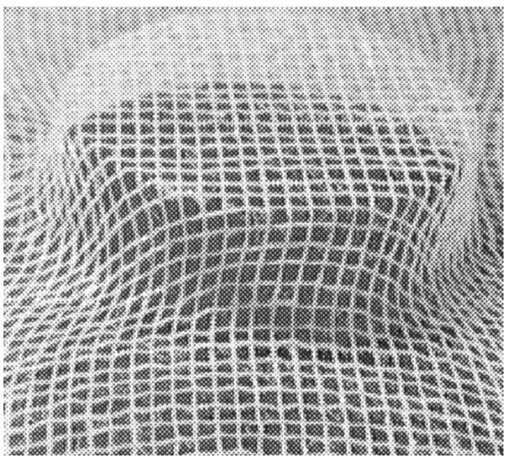

Figure 4. Fabric deformation without inter-fiber sliding, $D_1 = 34$ mm, $D_2 = 36$ mm, $h = 10$ mm, $r_2 = 2$ mm.

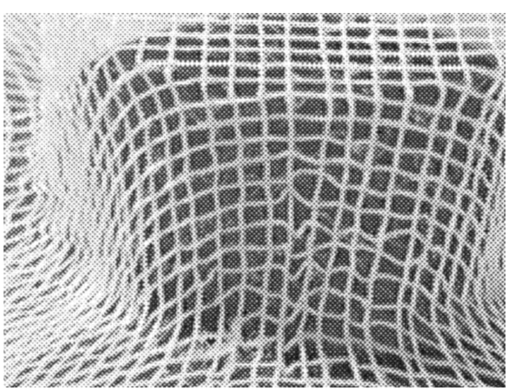

Figure 5. Buckling of yams on side surface, $D_1 = 34$ mm, $D_2 = 36$ mm, $h = 20$ mm, $r_2 = 2$ mm.

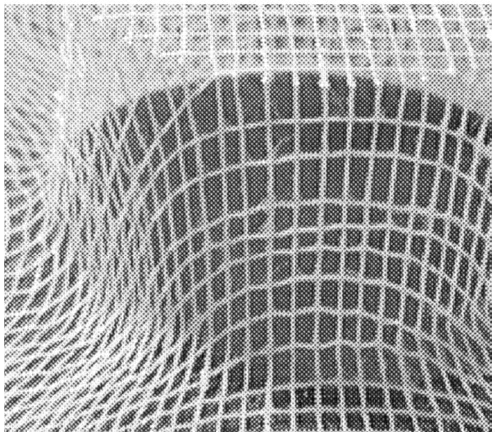

Figure 6. Inter-fiber sliding on side surface, $D_1 = 34$ mm, $D_2 = 36$ mm, $h = 20$ mm, $r_2 = 5$ mm.

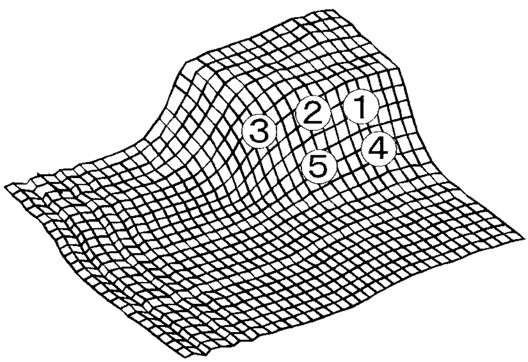

Region ①: Rectangular stitch region near the base of a cylinder.

Region ②: Medium shear deformation region near the base of a cylinder.

Region ③: Large shear deformation region on the side surface.

Region ④: Rectangular stitch region near the blank-holder.

Region ⑤: Medium shear deformation region near the blank-holder.

Figure 7. Measured points of inter-fiber sliding.

As shown in Fig. 7 (quarter part of fabrics), we measured the amount of inter-fiber sliding on the side surface, where only inter-fiber sliding occurs (we neglect inter-fiber sliding in the region where buckling of yarns occurs). Though yarns slide in both warp and weft directions, the amount of inter-fiber sliding cannot be distinguished by the sliding direction because of symmetry of the punch shape. We determined the amount of inter-fiber sliding by the larger displacement of an intersection in either the warp or the weft direction.

Relations between the radius r_2 and the amount of inter-fiber sliding are summarized in Figs 8–12. In these figures, the amount of inter-fiber sliding is higher for

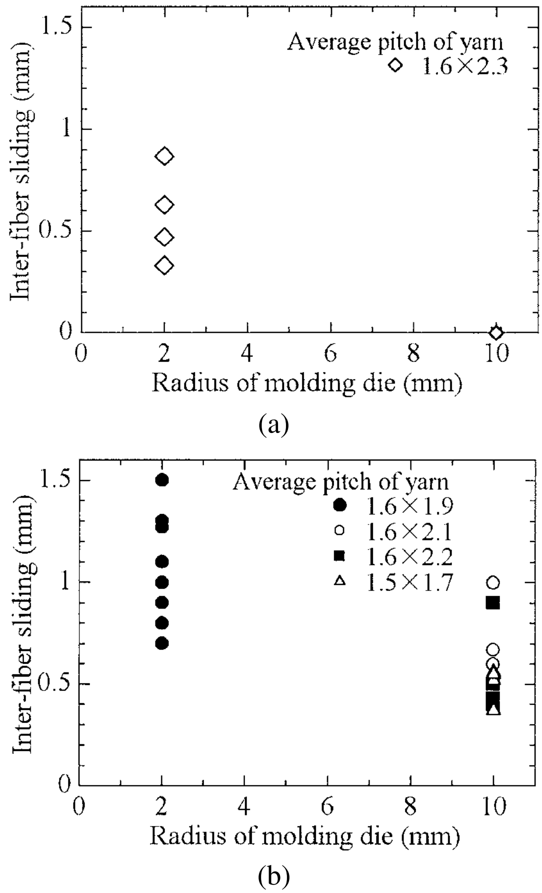

Figure 8. Inter-fiber sliding at region ① ($D_1 = 34$ mm). (a) $h = 10$ mm; (b) $h = 20$ mm.

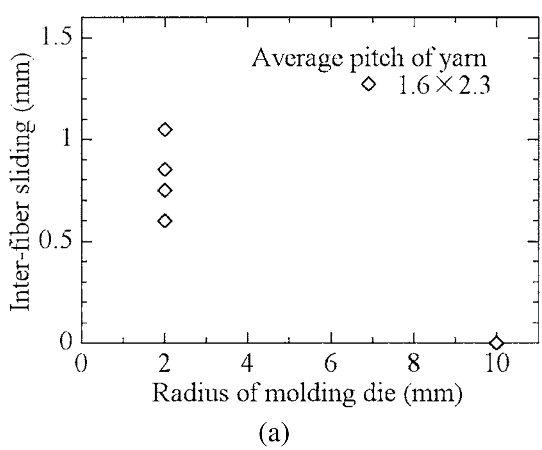

Figure 9. Inter-fiber sliding at region ② ($D_1 = 34$ mm). (a) $h = 10$ mm; (b) $h = 20$ mm.

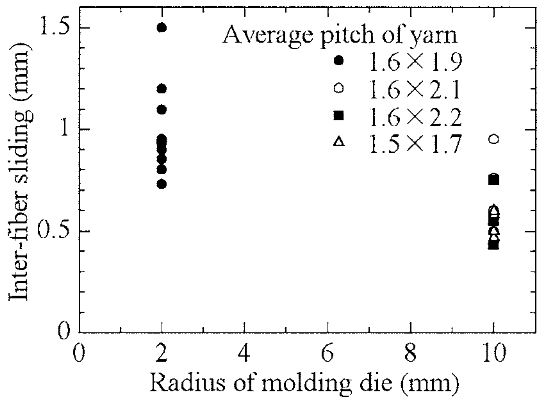

(b)

Figure 9. (Continued).

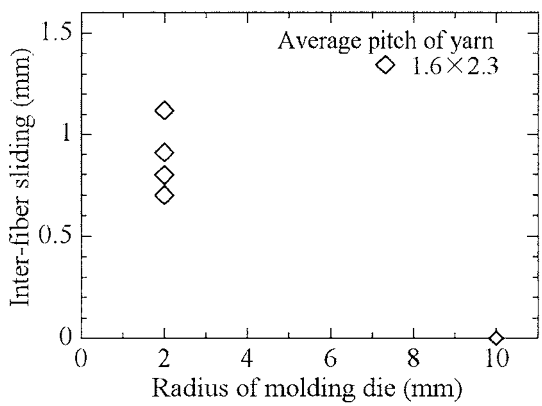

(a)

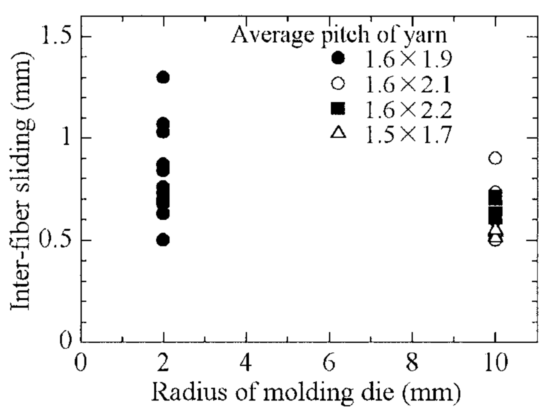

(b)

Figure 10. Inter-fiber sliding at region ③ ($D_1 = 34$ mm). (a) $h = 10$ mm; (b) $h = 20$ mm.

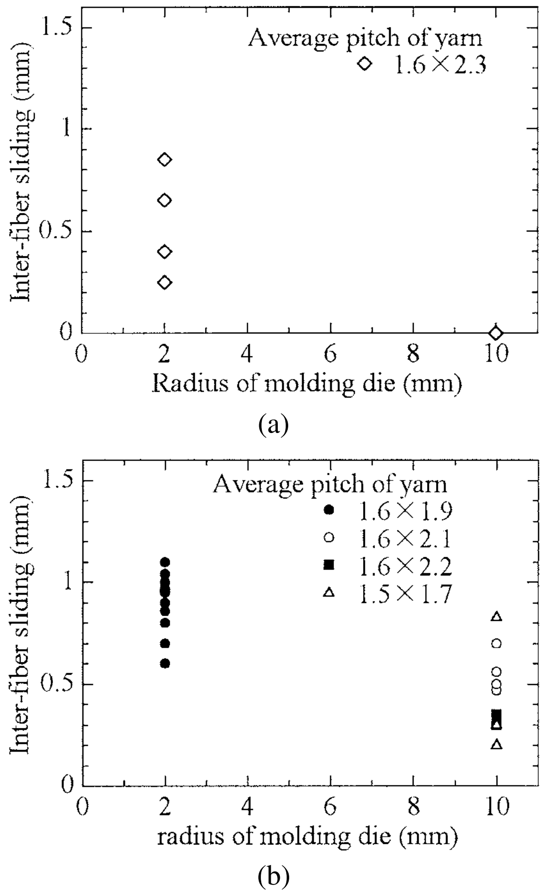

Figure 11. Inter-fiber sliding at region ④ ($D_1 = 34$ mm). (a) $h = 10$ mm; (b) $h = 20$ mm.

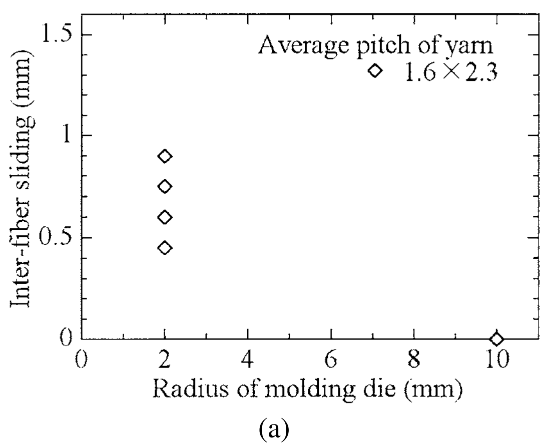

Figure 12. Inter-fiber sliding at region ⑤ ($D_1 = 34$ mm). (a) $h = 10$ mm; (b) $h = 20$ mm.

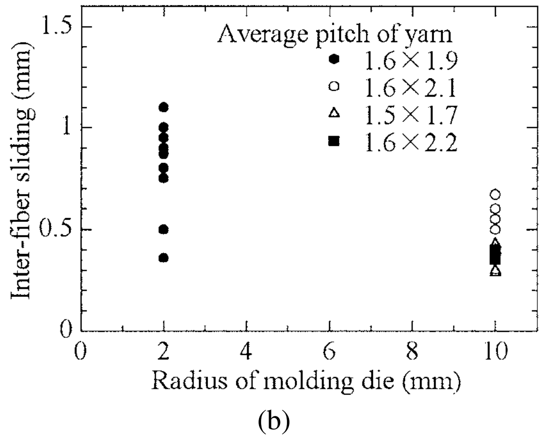

Figure 12. (Continued).

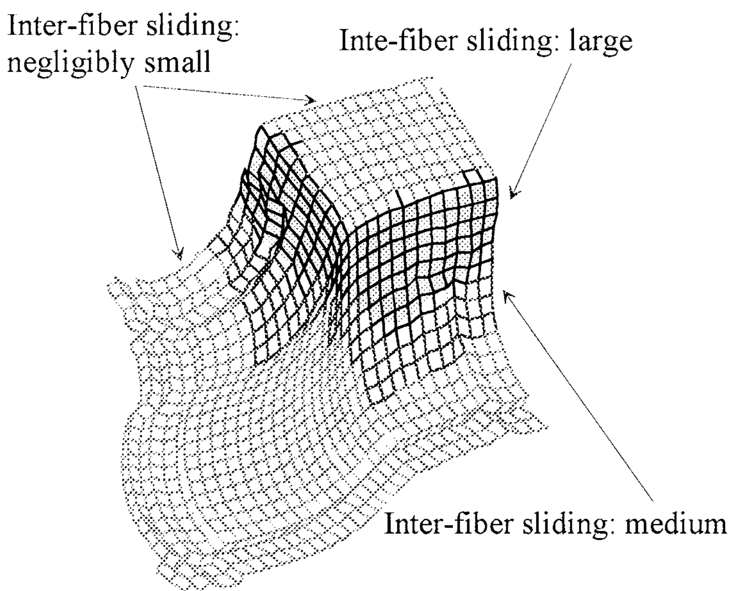

Figure 13. Distribution of inter-fiber sliding (h = 20 mm).

smaller r_2. Also, by comparing figures (a) and (b) in Figs 8–12, it can be concluded that the amount of inter-fiber sliding becomes larger when the punch traveling distance h increases.

Figure 13 shows the distribution of inter-fiber sliding for $h = 20$ mm (one-quarter part of the fabrics). The amount of inter-fiber sliding in the deep domain of a punch (around regions ① and ② shown in Fig. 7) is larger than that around the fringe of a punch (around regions ④ and ⑤ shown in Fig. 7).

4. COMPARISON BETWEEN SIMULATION AND EXPERIMENTS

We compared the simulation results based upon the pin-jointed network model and actual fabric deformation from experiments. Simulation using the FEM is quasi-statically performed with punch traveling. Figures 14a and b show the results and experimental results, respectively, under the condition of $h = 10$ mm. Figures 15a and b show the results for $h = 20$ mm.

When punch traveling is small, numerical results are in good agreement with experimental results. On the other hand, inter-fiber sliding and buckling of yarns occur in $h = 20$ mm. Macroscopic deformation of fabrics using the pin-

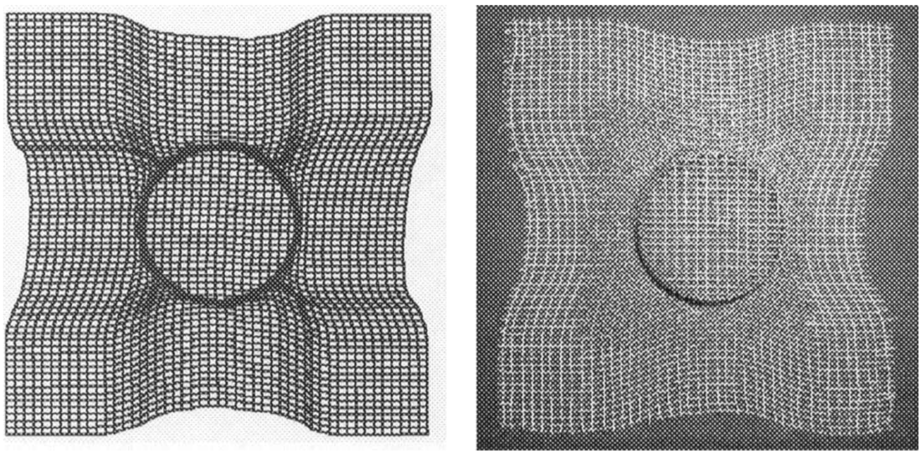

(a) (b)

Figure 14. Fabric deformation ($D_1 = 34$ mm, $r_2 = 2$ mm, $h = 10$ mm). (a) Numerical results. (b) Experimental results.

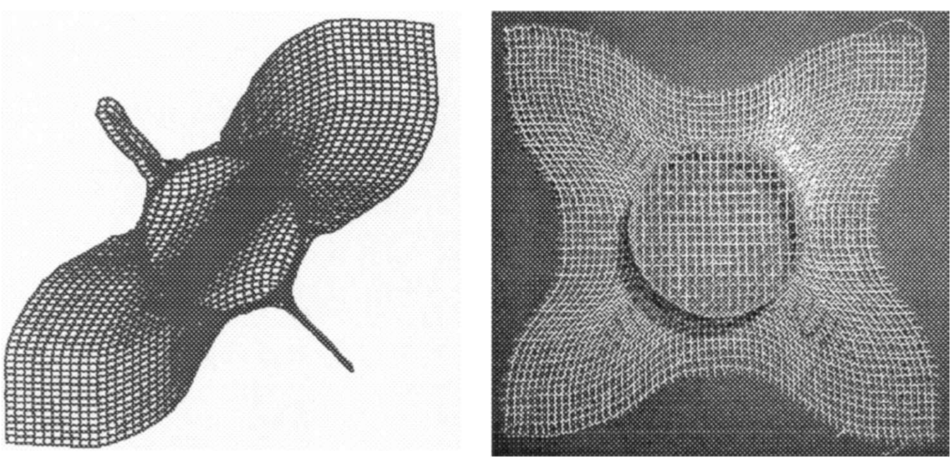

(a) (b)

Figure 15. Fabric deformation ($D_1 = 34$ mm, $r_2 = 2$ mm, $h = 20$ mm). (a) Numerical results. (b) Experimental results.

jointed model is different from actual experimental observation, that is, symmetry of deformation becomes less, with punch traveling. Since fabrics of the pin-jointed model cannot withstand inter-fiber sliding or buckling of yarns, fabrics tend to relax strain energy by the deformation of the whole fabrics. Furthermore, microscopic deformation of yarn orientation in the simulation is different from actual deformation, that is, large shear deformation occurs on the base of a cylindrical punch. Therefore, we should take into account both inter-fiber sliding and buckling of yarns in simulation.

5. CONCLUSIONS AND DISCUSSION

Numerical results may be quite different from actual deformation, if we neglect inter-fiber sliding and buckling in the simulation of the fabric shaping process. In the case of deep drawing with a semi-spherical punch, deformation without inter-fiber sliding and buckling of yarns is observed. Hence, research results obtained for semi-spherical shaping are usually valid. In the case of deep drawing with a cylindrical punch, deformation with inter-fiber sliding and buckling of yarns is observed, and we have obtained the following results.

(1) The amount of inter-fiber sliding becomes larger as the punch traveling distance increases.

(2) The radius of the molding die determines the transition area of fabrics from the fringe to the side surface. The large radius of the molding die effects smooth deformation of fabrics from the fringe to the side surface of the cylinder.

(3) Inter-fiber sliding on the base of a cylindrical punch and on the blank-holder is negligibly small. Inter-fiber sliding and buckling of yarns are observed on the side surface of a cylindrical punch. The amount of inter-fiber sliding in the deep domain of punch is larger than that around the fringe of the cylinder. This distribution of inter-fiber sliding suggests that inter-fiber sliding of fabric initiates around the fringe of the cylinder and increases with the punch traveling distance.

We observe inter-fiber sliding and buckling of yarns, simultaneously. Though it is difficult to determine the amount of buckling of yarns, we intend to identifying the factors inducing inter-fiber sliding or buckling of yarns in our future work.

One idea of how to estimate inter-fiber sliding [8] is based only on geometrical conditions, such as curvature of yarns. Inter-fiber sliding can be observed in the low yarn-curvature region ① shown in Fig. 7, and it corresponds to the pattern of single yarn bending shown in Fig. 1b. This pattern of inter-fiber sliding is believed to be strongly affected by the mechanical conditions. Since inter-fiber sliding is related to friction between fibers, we should take into account the mechanical conditions, such as tensile force in yarns, in future studies.

REFERENCES

1. C. Mack and H. M. Taylor, The fitting of woven cloth to surfaces, *J. Text. Inst.* **47**, 477–488 (1956).
2. F. Van der Ween, Algorithms for draping fabrics on doubly-curved surfaces, *Int. J. Num. Meth. Engng.* **31**, 1415–1426 (1991).
3. B. P. Van West and S. C. Luby, Fabric draping simulation in composites manufacturing, Part I: Description and application, *J. Adv. Mater.* **28**, 29–35 (1997).
4. J. Wang, R. Paton and J. R. Page, The draping of woven fabric preforms and prepregs for production of polymer composite components, *Composites A* **30**, 757–765 (1999).
5. P. Boisse, A. Cherouat, J. C. Gelin and H. Sabhi, Experimental study and finite element simulation of a glass fiber fabric shaping process, *Polym. Compos.* **16**, 83–95 (1995).
6. L. Dong, C. Lekakou and M. G. Bader, Solid-mechanics finite element simulations of the draping of fabrics: a sensitive analysis, *Composites A* **31**, 639–652 (2000).
7. Y. Arimitsu and T.-W. Chou, Modeling of yarn orientation and stress concentration in fabric shaping process, in: *Proc. of 23rd Int'l SAMPE Tech. Conf.*, Vol. 1, pp. 551–554 (1999).
8. C.-L. Lai and W.-B. Young, Modeling fiber slippage during the preforming process, *Polym. Compos.* **20**, 594–603 (1999).